PERGAMON

Water Research 37 (2003) 2043–2052

WATER RESEARCH

www.elsevier.com/locate/watres

Characterization of activated sludge flocs by confocal laser scanning microscopy and image analysis

Markus Schmid[a], Antoine Thill[b], Ulrike Purkhold[a], Marion Walcher[a], Jean Yves Bottero[b], Philippe Ginestet[c], Per Halkjær Nielsen[d,*], Stefan Wuertz[e], Michael Wagner[a]

[a] *Lehrstuhl für Mikrobiologie, Technische Universität München, Am Hochanger 4, D-85350 Freising, Germany*
[b] *Centre Européen de Recherche et d'Enseignement de Geosciences de l'Environnement, Europole de l'Arbois, B.P. 80, 13762 Les Milles Cedex, France*
[c] *CIRSEE-Ondeo Services, 38, rue du Président Wilson, 78230 Le Pecq, France*
[d] *Department of Environmental Engineering, Aalborg University, Sohngaardsholmsvej 57, DK-9000 Aalborg, Denmark*
[e] *Department of Civil and Environmental Engineering, University of California, Davis, One Shields Avenue, Davis, CA 95616, USA*

Received 3 July 2002; received in revised form 27 November 2002; accepted 4 December 2002

Abstract

In this study we present a new approach to determine volumes, heterogeneity factors, and compositions of the bacterial population of activated sludge flocs by 3D confocal imaging. After staining the fresh flocs with fluorescein-isothiocyanate, 75 stacks of images (containing approx. 3000 flocs) were acquired with a confocal laser scanning microscope. The self-developed macro 3D volume and surface determination for the KS 400 software package combined the images of one stack to a 3D image and calculated the real floc volume and surface. We determined heterogeneity factors like the ratio of real floc surface to the surface of a sphere with the respective volume and the fractal dimension (D_f). According to their significant influence on floc integrity and quality, we also investigated the chemical composition of flocs and quantified their bacterial population structure by using group-specific rRNA-targeted probes for fluorescence in situ hybridization. By a settling experiment we enriched flocs with poor settling properties and determined the above-mentioned parameters. This approach revealed shifts in floc volume, heterogeneity, and bacterial and chemical composition according to the settling quality of the flocs.

Keywords: Sludge settling; Confocal laser scanning microscopy (CLSM); Floc characterization; Fluorescence in situ hybridization (FISH)

1. Introduction

A prominent problem in wastewater treatment is poor settling properties of activated sludge flocs in the secondary clarifier. This often leads to a decreased performance of the wastewater treatment plant (WWTP) and in the worst case to environmental pollution.

The settling properties of activated sludge can be affected by a number of factors such as the median floc size and floc heterogeneity [1,2], by growth of filamentous or zoogloeal bacteria (e.g. [3,4]), and by the amount and composition of extracellular polymeric substances (EPS) in the sludge [5]. The relative importance of these factors is, however, not always well understood [6], so reliable methods to study settling characteristics and floc properties are important. The settling properties of the

*Corresponding author. Tel.: +45-96-35-8503; fax: +45-98-14-25-55.
E-mail address: phn@bio.auc.dk (P.H. Nielsen).

0043-1354/03/$ - see front matter
doi:10.1016/S0043-1354(02)00616-4

sludge are often characterized by measurement of the sludge volume index (SVI). However, this method only provides macroscopic settling properties [7]. Therefore, various studies have focused on methods for a more comprehensive characterization of activated sludge flocs.

Floc size distributions were previously determined by light microscopy (e.g. [8,9]). This approach revealed that most particles have a diameter lower than 5 μm but the major part of the volume is found by flocs with a diameter in the range of 68–183 μm. Since light microscopic studies are tedious, sizes of bacterial aggregates and their heterogeneity in terms of fractal dimensions were recently characterized by a light scattering approach [10]. This technique, though fast, provides only an indirect insight into physical floc properties with no information about the microbial community structure or EPS composition.

Since it was shown previously that confocal laser scanning microscopy (CLSM) is a suitable method for visualization of floc structure [11], we combined CLSM with image analysis to provide a direct determination of floc volume and architecture. We applied this approach to characterize activated sludge flocs with average and poor settling properties. CLSM-based applications for quantitative fluorescence in situ hybridization (FISH) were used to detect the population structure of the activated sludge flocs. The determination of the chemical composition of the flocs allowed us to detect differences in the physical structure, chemical composition, and in the microbial composition in poor settling flocs compared to the average flocs from WWTPs.

2. Materials and methods

2.1. Sampling

Samples were taken from the aeration basins from the plants listed in Table 1 and stored on ice.

2.2. Fractionation of activated sludge flocs

Samples were taken from the original sludges (time 0), which represent mixtures of flocs with different settling properties. For the separation of good and poor settling activated sludge flocs, each of the undiluted sludge samples was applied to a cylinder with a height of 22 cm and a diameter of 8 cm. The flocs were allowed to settle, so the poor settling flocs were enriched in the upper part of the supernatant. Previous settling experiments showed that an almost complete solid–liquid separation took place after about 20 min. Therefore, samples were taken after 20 min of settling using a glass pipette (without tip to avoid shearing effects) at a height of about 5 cm within the supernatant. Aliquots of these samples were immediately processed for analysis of the physical, chemical and biological parameters and compared to original samples.

2.3. Staining with fluorescein-isothiocyanate (FITC)

Samples were vortexed for 5 s prior to and after staining with FITC (Merk, Darmstadt, Germany) to destroy low-energy aggregation between flocs. Staining was performed for 3 h by addition of 25 μl of FITC-stock solution (1% FITC in dimethyl-formamide, Merck) to 1 ml of the native sample. All floc structures were best stained by FITC, which binds to molecules containing amino groups like the proteins and amino-sugars of cells and EPS. The Fluorescent Brightener 28 (Sigma-Aldrich, Steinheim, Germany) and the negative staining with fluoresceine (Sigma-Aldrich) yielded poorer results (data not shown). Excess dye was removed by carefully replacing the supernatant of the settled stained samples with fresh filtered sample liquid (0.2 μm). Samples were diluted with filtered sample liquid (0.2 μm) to gain single flocs and immediately viewed under the CLSM with a 40× objective (C-Apochromat W1.2, Zeiss, Jena, Germany). The basic slide setup described by Droppo et al. [12] was used for the acquisition but no agarose was needed to stabilize the flocs.

2.4. Fluorescence in situ hybridization

The oligonucleotide probes used are listed in Table 2. Further information to the probes is available at probeBase [13]. They were purchased as Cy3- and Cy5-labeled derivatives from Thermo Hybaid Interactiva

Table 1
Characteristics of analyzed municipal activated sludge samples

Sludge samples analyzed	PE	SVI	Suspended solids (g SSl^{-1})
Semitechnical plant Großlappen	ND	125	ND
WWTP Dietersheim; high load stage	1,000,000	72	3.7
WWTP Großlappen; high load stage	1,200,000	103	3.3
WWTP Poing	110,000	137	2.9

SVI and SS data were determined in the laboratories of the respective WWTP. PE = population equivalent and ND = not determined.

Table 2
Oligonucleotide probes and their specificity used in this study

Oligonucleotide probe	Specificity
Alf968	Many *Alphaproteobacteria*
Bet42a	*Betaproteobacteria*
Gam42a	*Gammaproteobacteria*
Pla46	*Planctomycetes*
CF319a	Many *Bacteroidetes*
Hgc69a	*Actinobacteria*
Lgcb + c[a]	Many *Firmicutes*
Eub338	Many but not all *Bacteria*
Eub338II	Bacterial lineages not covered by probe EUB338 and EUB338III
Eub338III	Bacterial lineages not covered by probe EUB338 and EUB338II

[a] An equimolar mixture of Lgcb and Lgcc was used for FISH.

Division (Ulm, Germany). Flocs were fixed and analyzed by FISH as described by Juretschko et al. [14].

2.5. Microscopy, image analysis, and quantification of probe target bacteria

For image acquisitions an LSM 510 scanning confocal microscope (Zeiss) equipped with an UV laser (351 and 364 nm), an Ar ion laser (458 and 488 nm), and two HeNe lasers (543 and 633 nm) was used together with the standard software package delivered with the instrument (version 2.1). For floc volume and surface determinations 3D image stacks were acquired with the CLSM and processed by the macro three-dimensional volume and surface determination (3DVASD) for the Carl Zeiss Vision KS400 software package, developed in this study. The floc volume was computed from the acquired 3D image stacks by enlargement of the pixels of each single slice by half of the slice distance in both directions of the z-axis. To separate background voxels from stained floc structure a voxel intensity threshold for each sludge sample was determined so voxels with an intensity below this threshold were not considered for volume measurement. Thus increasing threshold values starting from zero to 255 (maximum amount of intensity values in 8 bit grey images) in steps of five were applied to 10 randomly selected image stacks derived from one sample. Due to the high-intensity differences between background and stained flocs the measured volumes of one image stack stayed constant at thresholds from about 50 to about 120. The threshold applied to all image stacks was chosen from that range of threshold values in which each of the 10 stacks showed a constant volume. Resulting voxels, which touched each other in at least one plane, were defined as belonging to an individual structure. Additionally, voxels of non-stained enclosures within the structures were added to their volume. Voxels of these structures were counted and multiplied by the volume of one voxel given by the dimension of the pixels of the slices in the x- and y-direction and the slice distance. Structures touching the borders of the image stack were excluded from the measurement. Classes were defined in order to group the flocs according to their volume (Table 3). The overall surface of one individual structure was determined by adding voxel surface planes, which did not have other surface planes of stained voxels as neighbor. The surface information measured by the macro 3DVASD from CLSM acquired images was also used to determine the ratio of the real surface of a floc to the surface of a sphere with the respective volume (S_{floc}/S_{sphere}). Since the KS400 software package is not able to compute the original diameters of the flocs, diameters to the corresponding volume classes were determined with the following equation:

$$d_{floc} = \sqrt{S_{floc}/S_{sphere}} \times d_{ulvc}.$$

d_{floc} is the deduced diameter of an original floc with the volume of the upper limit of the respective volume class, S_{floc}/S_{sphere} the ratio of the original surface computed by the 3DVASD and the surface of a sphere with the respective volume of the floc (see below), and d_{ulvc} is the diameter of the sphere with the volume of the upper volume class limit.

The d_{floc} values were taken as the upper diameter class limit corresponding to the respective volume class and plant. Diameters and heterogeneity factors (S_{floc}/S_{sphere}) to the corresponding volume classes and plants are given in Table 3.

The fractal dimension (D_f) was deduced out of 20 randomly selected 2D image sections from acquired 3D image stacks of each sample by using the two-point correlation function mentioned in Thill et al. [15].

The filament indices were determined according to Jenkins et al. [3]. Quantification of probe-labeled bacterial populations was performed as described by Schmid et al. [16] and Daims et al. [17].

2.6. Determination of the chemical composition

The chemical composition of the sludges in terms of total protein, carbohydrate, DNA, and humic substances was measured as described by Frølund et al. [18].

3. Results

3.1. Evaluation of floc volume determination by CLSM and image analysis

To determine the number of flocs which need to be analyzed to get a reliable statistical floc volume

Table 3
Transfer of volume classes into the respective diameters

Volume classes (μm^3)	Dietersheim				Großlappen			
	0 min		20 min		0 min		20 min	
	S_{floc}/S_{sphere}	Diameter classes (μm)	S_{floc}/S_{sphere}	Diameter classes (μm)	S_{floc}/S_{sphere}	Diameter classes (μm)	S_{floc}/S_{sphere}	Diameter classes (μm)
17–32	2.00	4.51–5.57	2.12	4.65–5.74	2.16	4.69–5.79	2.22	4.75–5.86
33–64	2.01	5.58–7.03	2.13	5.75–7.25	2.19	5.80–7.34	2.29	5.87–7.51
65–128	1.98	7.04–8.79	2.13	7.26–9.13	2.27	7.35–9.43	2.41	7.52–9.71
129–256	2.02	8.80–11.2	2.11	9.14–11.5	2.32	9.44–12.0	2.56	9.72–12.61
257–512	2.09	11.2–14.3	2.16	11.5–14.6	2.38	12.0–15.3	2.72	12.6–16.4
513–1024	2.07	14.4–18.0	2.32	14.6–19.1	2.44	15.3–19.6	2.91	16.4–21.3
1025–2048	2.11	18.0–22.9	2.31	19.0–24.0	2.61	19.6–25.5	3.10	21.4–27.8
2049–4096	2.39	22.9–30.7	2.36	24.0–30.5	2.86	25.5–33.6	3.10	27.8–35.0
4097–8192	2.47	30.7–39.3	2.72	30.5–41.2	3.26	33.6–45.2	3.02	35.0–43.5
8193–16,390	2.26	39.3–47.4	2.69	41.24–51.7	3.52	45.2–59.1	3.83	43.5–61.7
16,390–32,770	2.56	47.4–63.6	2.82	51.7–66.7	4.38	59.1–83.1	4.36	61.7–82.9
32,770–65,540	2.81	63.6–83.9	3.56	66.7–94.3	5.00	83.1–112	4.61	82.9–107
65,540–131,100	3.24	83.9–113	4.31	94.3–131	4.91	112–140	5.39	107 –146
131,100–262,100	3.63	113–151	5.31	131–183	5.64	140–189	7.30	146–215
262,100–524,300	4.88	151–221	5.44	183–233	6.78	189–261	9.13	215–302
524,300–1,049,000	5.43	221–294	6.50	233–321	8.28	261–363	11.38	302–425
1,049,000–2,097,000	6.96	294–419	7.58	321–437	8.64	363–467	12.34	425–558

distribution, the volumes of 600, 3000, 6000, and 15,000 randomly selected flocs originating from the same activated sludge sample from Dietersheim WWTP were measured. Pronounced differences were observed in the floc volume distributions inferred from 600, 3000 and 6000 analyzed flocs. Almost identical volume distributions were obtained from 6000 and 15,000 measured flocs (data not shown). The 6000 flocs corresponded to approx. 75 confocal images. Consequently, the time required for sample treatment (staining, wash steps, etc.) and image acquisition (without data analysis) was approx. 7 h for a single sample. To investigate the influence of storage on activated sludge, an aliquot of the sludge from Dietersheim WWTP was stained and observed immediately after sampling. Other aliquots were examined after storage times of 6 h, 1, 2, 3 and 5 days at 4°C, respectively. For each analysis, 6000 flocs were recorded at room temperature. The storage did not cause any pronounced shifts in the volume distributions.

The largest distance between confocal optical sections, which can be applied without significant decrease of the accuracy of the analysis, was defined by taking 20 CLSM stack images of an activated sludge sample using 1 μm distance intervals between the optical sections (distances <1 μm were not analyzed since they are not practicable due to bleaching effects caused by the extended excitation time). After data acquisition, individual sections were removed from each stack image to obtain modified data sets with distances between the sections of 2, 4, and 8 μm. The use of section distances of 1, 2, and 4 μm resulted in only marginal variations in the determined floc volumes and distributions. The total volumes of all measured flocs using 1, 2, and 4 μm section distance, respectively, differed only by 3.5%. However, increase of section distance to 8 μm led to significant alterations of floc volumes and distributions. This is also reflected by a 25% overestimation of the total floc volume using 8 μm as section distance.

3.2. Physical floc properties

The physical floc properties were determined for the semitechnical plant in Großlappen and the Dietersheim WWTP. Generally, the small flocs were most abundant [below 256 μm^3 (diameter of about 9 μm; Table 3) Figs. 1, 2A and B], while the large ones comprised almost the complete volume [above 131,073 μm^3 (diameter above about 140 μm; Table 3)]. The poor settling flocs remaining in the supernatant after 20 min of settling in Dietersheim were slightly more voluminous (Fig. 2A) and the abundance of small flocs decreased (Fig. 2B). In contrast, the poor settling flocs in Großlappen showed a shift to smaller volumes in the larger volume classes [above 131,073 μm^3 (diameter above about 140 μm; Table 3); Fig. 2A]. A significant increase in the number of small flocs was not visible (Fig. 2B).

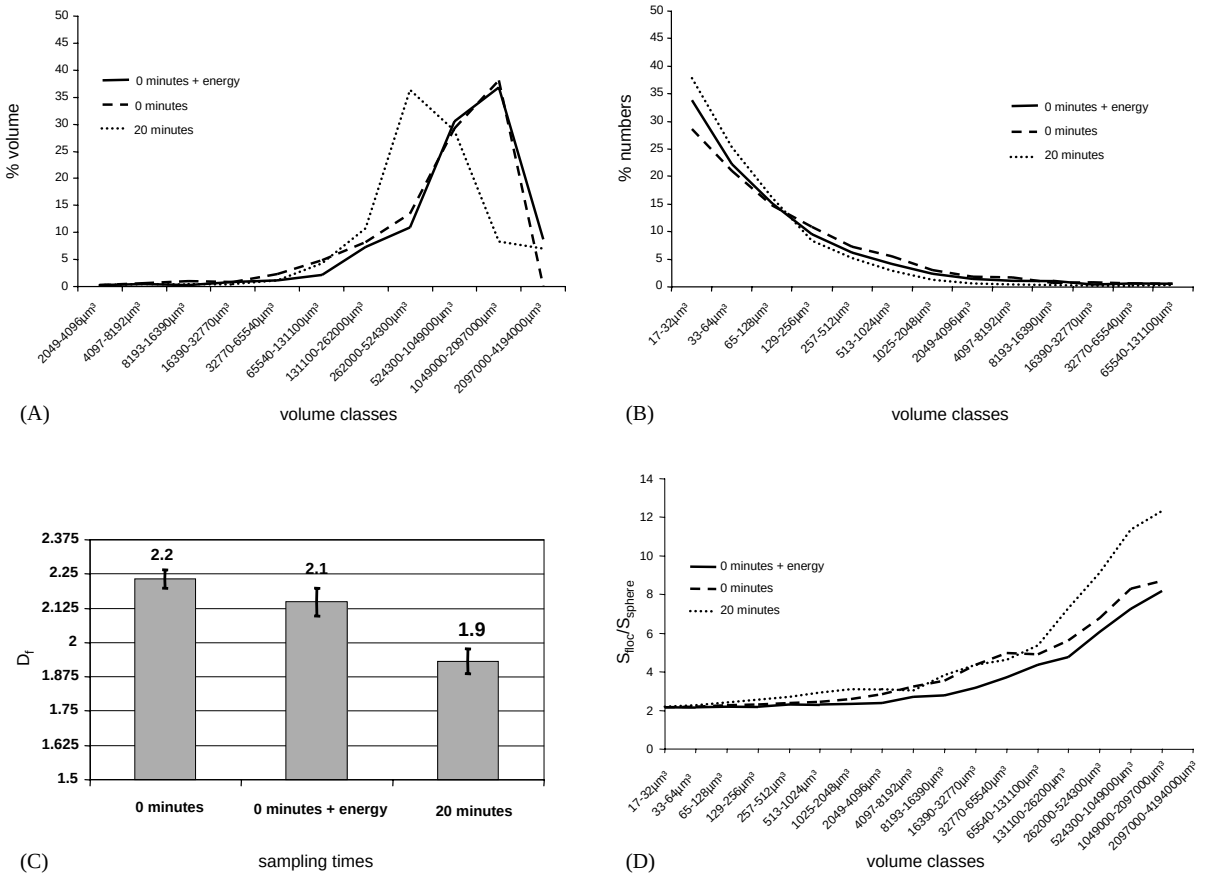

Fig. 1. (A, B) Volume distribution of activated sludge flocs from Großlappen after enrichment for flocs with poor settleability and application of energy (by vortexing to break up weak adhesions of flocs), respectively. For each volume class the relative contribution to the total volume of all flocs (A) and the relative contribution to the total number of all flocs (B), which were analyzed, are given. (C) D_f values of activated sludge flocs after enrichment for flocs with low settleability and application of energy, respectively. For each analysis, the D_f of 20 activated sludge flocs was determined. Error bars indicate the standard error. (D) S_{floc}/S_{sphere} of activated sludge flocs after enrichment for flocs with poor settleability and application of energy, respectively.

The fractal dimension (D_f) of the poor settling flocs had mean values (1.9 for Großlappen and 1.8 for Dietersheim) lower than the D_f of the original sludge flocs (2.2 for Großlappen and 2.1 for Dietersheim) indicating that the poor settling flocs were slightly more heterogeneous (Figs. 1C and 2C). This is also supported by measurement of the ratio of the floc surface to the surface of a sphere with an identical volume (S_{floc}/S_{sphere}), which showed a marked increase for poor settling flocs in both plants (Figs. 1D and 2D).

3.3. Chemical composition and population structure of activated sludge

The chemical composition of the solids was determined in the activated sludge samples from the three WWTPs (Table 4). In all plants the relative carbohydrate content decreased while the DNA content increased when the poor settling flocs were enriched. In contrast, the change in the content of humic substances and proteins did not show a general pattern as it increased, decreased or remained constant in the WWTPs investigated.

Group-specific probes were applied to investigate the microbial population structure of the activated sludge of the different WWTPs (Fig. 3). Activated sludge from all three plants was dominated by *Betaproteobacteria* and *Actinobacteria* (Fig. 3). In Poing also *Firmicutes* were numerous. In medium amounts, members of the *Alpha-* and *Gammaproteobacteria* could be detected in Dietersheim and Poing (Figs. 3A–C). The Großlappen sludge contained the most heterogeneous bacterial population (Fig. 3B) and a relatively high proportion of the bacteria could not be identified by any of the probes applied (18%).

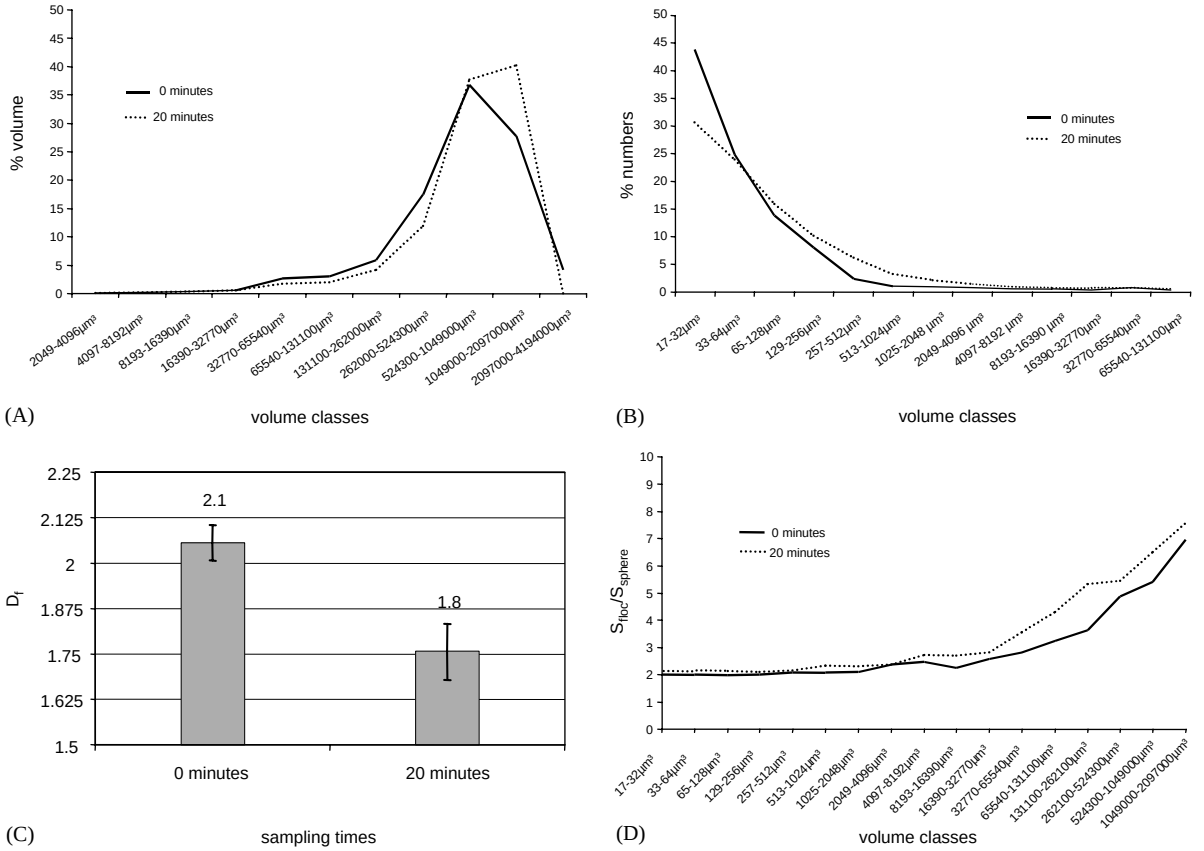

Fig. 2. (A, B) Volume distribution of Dietersheim activated sludge flocs after enrichment for flocs with poor settleability. For each volume class the relative contribution to the total volume of all flocs (A) and the relative contribution to the total number of all flocs (B), which were analyzed, are given. (C) D_f values of activated sludge flocs after enrichment for flocs with poor settleability. For each analysis, the D_f of 20 activated sludge flocs was determined. Error bars indicate the standard error. (D) S_{floc}/S_{sphere} of activated sludge flocs of Dietersheim after enrichment for flocs with poor settleability and application of energy, respectively.

Table 4
Percental share of DNA, carbohydrates, proteins, and humic substances of the total chemical composition of activated sludge flocs of WWTPs Dietersheim, Großlappen, and Poing prior to and after enrichment for flocs with bad settling properties

		DNA	Carbohydrates	Humic substances	Proteins
Dietersheim	0 min	0.43	10.8	26.4	62.4
	20 min	0.92	6.3	34.3	58.5
Großlappen	0 min	0.18	15.9	24.9	59.0
	20 min	2.64	14.2	27.2	55.9
Poing	0 min	0.20	17.8	28.6	53.4
	20 min	1.20	12.8	27.0	59.1

After enrichment for poor settling sludge two major shifts in the population could be observed in the Dietersheim sludge (Fig. 3A). The *Betaproteobacteria* decreased from about 62% to 40% and *Alphaproteobacteria* from about 15% to 7%.

In poor settling sludge from Großlappen all bacteria could be detected with the applied group-specific oligonucleotide probes and the relative abundance of the *Alpha-*, *Beta-* *Gammaproteobacteria* and *Firmicutes* raised accordingly.

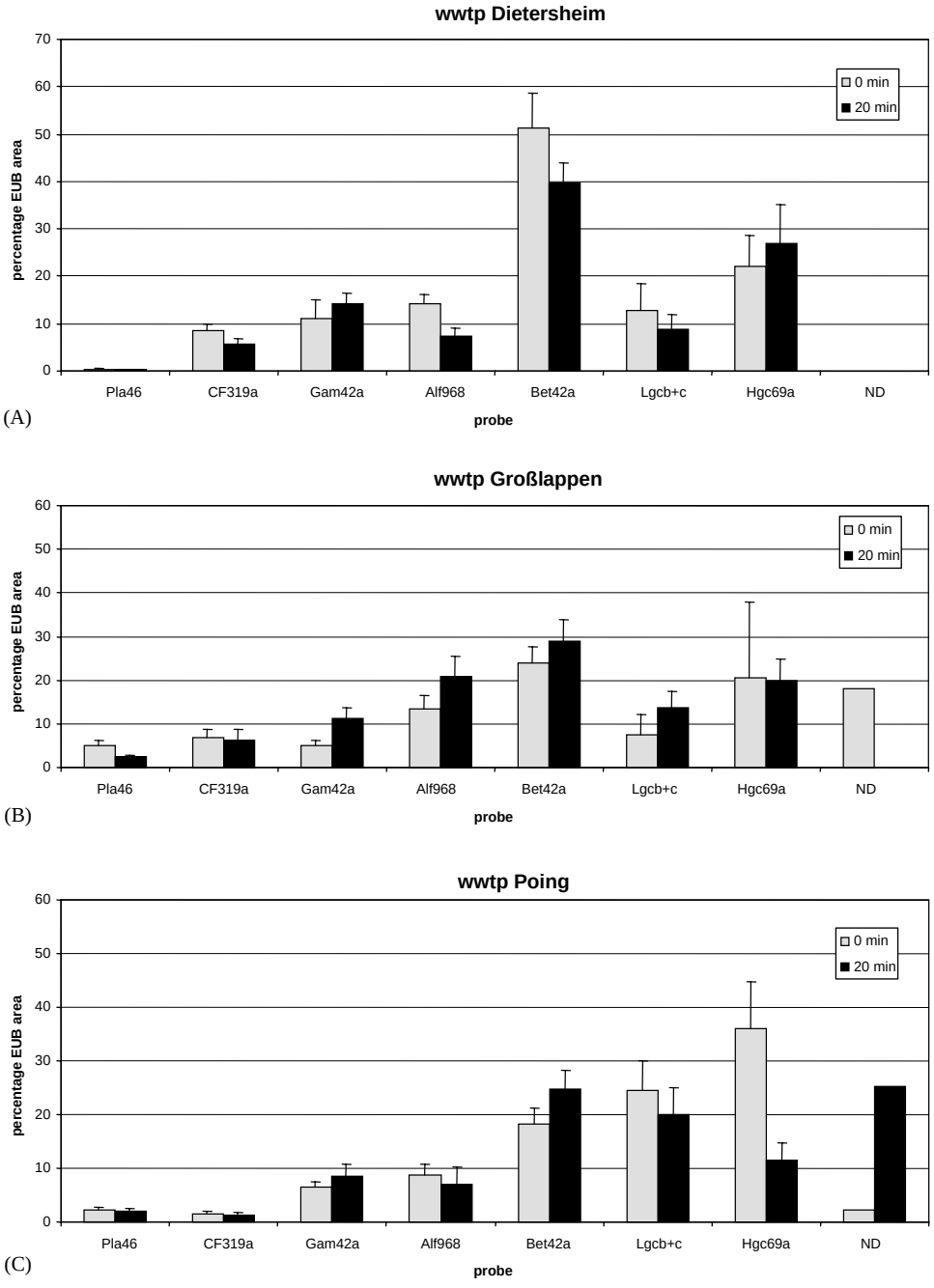

Fig. 3. Microbial population structure of the activated sludge samples prior to and after enrichment for flocs with poor settling properties of WWTPs: (A) Dietersheim, (B) Großlappen and (C) Poing (for probe details please refer to Table 2). ND = not determined = bacterial population detected by the EUB probe mix but not affiliated to any of the bacterial groups for which specific probes were applied. Error bars indicate the standard error.

In the poor settling flocs from Poing the abundance of *Actinobacteria* dropped significantly (from 35% to 10%) after enrichment for poor-settling flocs. A large fraction (about 25%) of the bacterial population in the poor settling flocs could be detected only with the EUB probe mixture (Fig. 3C) and must thus be affiliated with bacterial lingeages for which no specific probes were applied.

Additionally, a general shift in the filament index to higher values (from 2 to 4 for Dietersheim and

Großlappen, and from 3 to 5 for Poing, respectively) could be observed for all WWTPs after enrichment for poor settling flocs.

4. Discussion

4.1. Floc volume determined by CLSM and image analysis

Compared to previous approaches to determine floc structure [10,19] the use of the CLSM is relatively fast and flexible. To obtain statistically reliable results 75 stacks with ca. 6000 flocs had to be acquired. It took a few hours which potentially could have influenced the floc structure, but as long as the sludge was cooled down, not stirred or not supplied with substrate, no changes could be detected during data acquisition or during a couple of days storage.

The accuracy of the floc volume determinations depends on the distances between the optical sections. The lower limit for the CLSM is 0.1 μm, but we found a section distance of 4 μm as an optimal compromise as smaller section distances resulted in (i) time intensive measurements, (ii) extended excitation times causing strong fluorochrome bleaching, and (iii) accumulation of large amounts of digital data.

Previous studies used diameter classes (e.g. [8,9]) rather than volume classes for the description of floc sizes. This method does not take into account that it deals with 3D structures and volume measurement is in this respect more accurate. However, the software applied in this study was not able directly to compute the equivalent diameters and therefore they had to be deduced from volume and heterogeneity data in order to compare with previously published data (see materials and methods section). It should be noted that these diameter values only allow a relatively rough comparison and should not be taken as absolute values.

4.2. Physical and chemical properties of activated sludge flocs

The typical floc size distribution is described in various publications (e.g. [8,9]) as a curve with a peak at small particles with a diameter of about 0.5–5 μm and one for large particles with a diameter of 30–1000 μm. Our results generally obey these findings, but pronounced differences in the floc size distributions and heterogeneity could be found after enrichment for poor settling sludge.

The poor settling flocs in Großlappen were characterized to be smaller flocs compared to the original sludge. Furthermore, there was a significant increase in the number of filaments as indicated by a change in filament index from 2 (few filaments) to 4 (many filaments). In Dietersheim only a slight shift in the floc volume could be detected while the number of filaments also increased significantly. Thus, there seemed to be an enrichment of filaments in the poor settling flocs in both plants.

In contrast to the volume determinations, consistent trends were observed for the fractal dimension of the flocs during enrichment for flocs with poor settleability. D_f of the flocs with a bad settleability were in both plants characterized by a more heterogeneous structure (D_f of 1.9 and 1.8, respectively; Figs. 1C and 2C) than the flocs from the original activated sludges (D_f of 2.2 and 2.1, respectively; Figs. 1C and 2C). The ratio of the floc surface to the surface of a sphere of an identical volume (S_{floc}/S_{sphere}) also describes the structural heterogeneity of activated sludge flocs. Interestingly, the overall value for S_{floc}/S_{sphere} of large flocs was significantly higher for Großlappen than for Dietersheim indicating a higher heterogeneity in the overall floc structure in Großlappen. This finding is not supported by the D_f values. In this respect it seems that the D_f reflects a tendency within one sludge plant, but cannot be used to compare different plants. It is tempting to speculate that a higher S_{floc}/S_{sphere} of large flocs is indicative for a higher SVI since the sludge from the Großlappen plant has a higher SVI (125) compared to the sludge from Dietersheim (72). The results might indicate that the difference in the overall settling properties as indicated by SVI (Großlappen 125 and Dietersheim 72) was due mainly to larger and more heterogeneous flocs.

The chemical analysis of the activated sludge showed a composition similar to other sludge types with protein as the major compound [6]. For all WWTPs, the relative carbohydrate content decreased and the relative DNA content increased if flocs with poor settleability were enriched. Changes in the content of humic substances and proteins in all WWTPs investigated seemed not to obey general rules. In previous studies it was shown that a high content of uronic acids is likely to be linked to a better settleability of flocs [20]. This could indicate that carbohydrate fraction of the biomass is enriched in good settling flocs. However, this assumption is inconsistent with the observed increase in DNA content in poor settling flocs. Thus, there may not exist any substantial chemical difference between the different floc types, or the categories total humic substances, carbohydrates, proteins and DNA are too broad a measure to provide sufficient resolution for linking chemical composition with floc sizes or floc structure.

4.3. Population structure of activated sludge flocs

FISH is a powerful tool for cultivation-independent identification of microorganisms. In combination with CLSM and digital image analysis, quantitative data of the composition of the microbial populations in

activated sludge flocs and biofilms can be obtained (e.g. [17,14,21]). In accordance with previous investigations (e.g. [22,23]) two of the activated sludge samples analyzed were dominated by *Betaproteobacteria*, which encompass most lithoautotrophic ammonia-oxidizers, *Zoogloea spp.*, *Sphaerotilus natans*, and *Azoarcus* spp. The latter genus was recently identified to encompass important denitrifiers in WWTPs [14]. *Actinobacteria* (e.g. *Nocardia* spp.; *Rhodococcus* sp.) also played a numerically important role in all samples analyzed and dominated in the Poing plant.

Pronounced shifts in the microbial population structure of the activated sludge flocs from three different WWTPs were observed after enrichment for poor settling flocs (Fig. 3). These shifts demonstrate links between the settling property of a floc and its microbial community composition. However, using the group-specific probes the community shifts induced by enrichment for poor settling flocs did not follow a general tendency. This finding most likely reflects that different bacterial populations influence the settling properties in the different WWTPs investigated. Furthermore, the application of group-specific probes does not allow one to observe population shifts within the respective bacterial groups. Future research should attempt to apply the full-cycle rRNA approach [24,14] for a comparative analysis of the microbial community composition of activated sludge prior to and after enrichment for poor settling flocs. This approach will almost certainly allow one to identify bacterial key populations enriched in flocs with good or bad settleability.

5. Conclusions

1. CLSM in combination with image analysis is a powerful method for direct determination of the floc volume, heterogeneity factors and the population structure of activated sludge flocs.
2. The importance of physical, chemical and microbial floc properties to describe the settleability varies for each WWTP. Therefore, a detailed understanding of variations in sludge settling properties in different WWTPs, e.g. a certain malfunction, requires information about all factors.
3. Significant changes specific for each WWTP in the microbial population structure of original flocs and poor settling flocs could be observed (e.g. high amounts of *Actinobacteria* in the original sludge of Poing dropped to about a third of the original value after enrichment for poor settling flocs).

Acknowledgements

This work was supported by a grant of the CIRSEE-Ondeo Services to M. Wagner and the Sonderforschungsbereich 411 from the Deutsche Forschungsgemeinschaft (Project A2 of M. Wagner; Research Center for Fundamental Studies of Aerobic Biological Wastewater Treatment).

References

[1] Sadalgekar VV, Mahajan BA, Shaligram AM. Evaluation of sludge settleability by floc characteristics. J Water Pollut Control Fed 1988;60:1862–3.
[2] Andreadakis AD. Physical and chemical properties of activated sludge floc. Water Res 1993;27:1707–14.
[3] Jenkins D, Richard MG, Daigger GJ. Manual on the causes and control of activated sludge bulking and foaming, 2nd ed. Michigan, USA: Lewis Publishers, 1993.
[4] Wanner J. Activated sludge bulking and foaming control. Lancaster, USA: Technomic Publishing Company, 1994.
[5] Urbain V, Block JC, Manem J. Bioflocculation in activated sludge: an analytical approach. Water Res 1993;27:829–38.
[6] Nielsen PH. The activated sludge floc. In: Bitton G, editor. Encyclopedia in environmental microbiology. Chichester, England: Wiley. 2002.
[7] Dick RI, Vesilind PA. The sludge volume index—what is it? J Water Pollut Control Fed 1969;41:1285–91.
[8] Li D-H, Ganczarczyk JJ. Size distribution of activated sludge flocs. Res J Water Pollut Control Fed 1991;63:806–14.
[9] Jorand F, Zartarian F, Thomas F, Block JC, Bottero JY, Villemin G, Urbain V, Manem J. Chemical and structural (2D) linkage between bacteria within activated sludge flocs. Water Res 1995;29:1639–47.
[10] Guan J, Waite TD, Amal R. Rapid structure characterization of bacterial aggregates. Environ Sci Technol 1998;32:3735–42.
[11] Liss SN, Droppo IG, Flannigan DT, Leppard GG. Floc architecture in wastewater and natural riverine systems. Environ Sci Technol 1996;30:680–6.
[12] Droppo IG, Flannigan DT, Leppard GG, Jaskot C, Liss SN. Floc stabilization for multiple microscopic techniques. Appl Environ Microbiol 1996;62:3508–15.
[13] Loy A, Horn M, Wagner M. ProbeBase—an online resource for rRNA-targeted oligonucleotide probes. Nucleic Acids Res. 2003;31(1):514–6.
[14] Juretschko S, Loy A, Lehner A, Wagner M. The microbial community composition of a nitrifying-denitrifying activated sludge from an industrial sewage treatment plant analyzed by the full-cycle rRNA approach. Syst Appl Microbiol 2002;25:84–99.
[15] Thill A, Wagner M, Bottero JY. Confocal scanning laser microscopy as a tool for the determination of 3D floc structure. J Colloid Interface Sci 1999;220:465–7.
[16] Schmid M, Twachtmann U, Klein M, Strous M, Juretschko S, Jetten M, Metzger JW, Schleifer K-H, Wagner M. Molecular evidence for genus level diversity of bacteria capable of catalyzing anaerobic ammonium oxidation. Syst Appl Microbiol 2000;23:93–106.

[17] Daims H, Ramsing NB, Schleifer K-H, Wagner M. Cultivation-independent, semiautomatic determination of absolute bacterial cell numbers in environmental samples by fluorescence in situ hybridization. Appl Environ Microbiol 2001;67:5810–8.

[18] Frølund B, Palmgren R, Keiding K, Nielsen PH. Extraction of exopolymers from activated sludge using a cation exchange resin. Water Res 1996;30:1749–58.

[19] Zartarian F, Mustin C, Villemin G, Ait-Ettager T, Thill A, Bottero JY, Mallet JL, Snidaro D. Three-dimensional modeling of an activated sludge floc. Langmuir 1997;13: 35–40.

[20] de Beer D, O'Flaharty V, Thaveesri J, Lens P, Verstraete W. Distribution of extracellular polysaccharides and flotation of anaerobic sludge. Appl Microbiol Biotechnol 1996;46:197–201.

[21] Wagner M, Hutzler P, Amann R. 3-D analysis of complex microbial communities by combining confocal laser scanning microscopy and fluorescence in situ hybridization FISH. In: Wilkinson MHF, Schut F, editors. Digital image analysis of microbes. Chichester, England: Wiley, 1998. p. 467–86.

[22] Snaidr J, Amann R, Huber I, Ludwig W, Schleifer K-H. Phylogenetic analysis and in situ identification of bacteria in activated sludge. Appl Environ Microbiol 1997;63: 2884–96.

[23] Wagner M, Amann R, Lemmer H, Schleifer KH. Probing activated sludge with oligonucleotides specific for *Proteobacteria*: inadequacy of culture-dependent methods for describing microbial community structure. Appl Environ Microbiol 1993;59:1520–5.

[24] Amann RI, Ludwig W, Schleifer K-H. Phylogenetic identification and *in situ* detection of individual microbial cells without cultivation. Microbiol Rev 1995;59: 143–69.